J|A|C|S
ARTICLES
Published on Web 02/24/2007

Fluorescent HIV-1 Dimerization Initiation Site: Design, Properties, and Use for Ligand Discovery

Victor K. Tam, Denise Kwong, and Yitzhak Tor*

Contribution from the Department of Chemistry and Biochemistry, University of California, San Diego, La Jolla, California 92093-0358

Received October 23, 2006; E-mail: ytor@ucsd.edu

Abstract: The HIV-1 Dimerization Initiation Site (DIS) is an intriguing, yet underutilized, viral RNA target for potential antiretroviral therapy. To study the recognition features of this target and to provide a quantitative, rapid, and real-time tool for the discovery of new binders, a fluorescence-based assay has been constructed. It relies on strategic incorporation of 2-aminopurine, an isosteric fluorescent adenosine analogue, into short hairpin RNA constructs. These oligomers self-associate to form a kissing loop that thermally rearranges into a more stable extended duplex, thereby mimicking the association and structural features of the native RNA sequence. We demonstrate the ability of two fluorescent DIS constructs, DIS272(2AP) and DIS273-(2AP), to report the binding of known DIS binders via changes in their emission intensity. Binding of aminoglycosides such as paromomycin to DIS272(2AP) results in significant fluorescence enhancement, while ligand binding to DIS273(2AP) results in fluorescence quenching. These observations are rationalized by comparison to the sequence-analogous bacterial A-site, where the relative emission of the fluorescent probe is dependent on the placement of the flexible purine residues inside or outside the helical domain. Analysis of binding isotherms generated using DIS272(2AP) yields submicromolar EC_{50} values for paromomycin (0.5 ± 0.2 μM) and neomycin B (0.6 ± 0.2 μM). Other neomycin-family aminoglycosides are less potent binders with neamine, the core pharmacophore, displaying the lowest affinity of 21 ± 1 μM. Screening of additional aminoglycosides and their derivatives led to the discovery of new, previously unreported, aminoglycoside binders of the HIV DIS RNA, among them butirosin A (5.5 ± 0.6 μM) and apramycin (7.6 ± 1.0 μM). A conformationally constrained neomycin B analogue displays a rather high affinity to the DIS (1.9 ± 0.2 μM). Among a series of nucleobase aminoglycoside conjugates, only the uracil derivatives display a measurable affinity using this assay with EC_{50} values in the 2 μM range. In addition, similarity between the solution behavior of HIV-1 DIS and the bacterial decoding A-site has been observed, particularly with respect to the intra- and extra-helical residence of the conformationally flexible A residues within the bulge. Taken together, the observations reported here shed light on the solution behavior of this important RNA target and are likely to facilitate the design of new DIS selective ligands as potential antiretroviral agents.

Introduction

According to figures generated by the WHO and UNAIDS, more than 40 million people worldwide currently live with HIV/AIDS. About 4 million people have been newly infected in 2005, and nearly 3 million HIV/AIDS-related deaths have been documented.[1] While it appears the epidemic has essentially been controlled in large parts of the western world, the global prognosis appears grim. Projections suggest the epidemic could at least double (and possibly triple) by the end of the decade. This forecast seems particularly bleak for heavily populated countries.

The development of antiretroviral therapy against AIDS has been a major challenge since the discovery of the human immunodeficiency virus.[2] Early successes with nucleoside and non-nucleoside reverse transcriptase (RT) inhibitors, as well as the development of protease inhibitors, have facilitated a highly active antiretroviral therapy (HAART), where a combination of drugs is simultaneously administered.[3,4] Nevertheless, the rapid appearance of resistant HIV-variants,[5−12] adverse effects,[13,14] and recent indications for HIV "superinfections"[15,16]

(1) "UNAIDS: 2006 Report on the global AIDS epidemic". Available at http://www.unaids.org.
(2) Mohan, P.; Baba, M. *Anti-AIDS drug development: challenges, strategies and prospects*; Harwood Academic Publishers: Chur, Switzerland; U.S., 1995.
(3) Moore, R. D.; Chaisson, R. E. *AIDS* **1999**, *13*, 1933−1942.
(4) Baliant, G. A. *Pharmacol. Ther.* **2001**, *89*, 17−27.
(5) Garcia-Lerma, J. G.; Heneine, W. *J. Clin. Virol.* **2001**, *21*, 197−212.
(6) Durant, J.; Clevenbergh, P.; Halfon, P.; Delgiudice, P.; Porsin, S.; Simonet, P.; Montagne, N.; Boucher, C. A.; Schapiro, J. M.; Dellamonica, P. *Lancet* **1999**, *353*, 2195−2199.
(7) Loveday, C.; Devereux, H.; Huckett, L.; Johnson, M. *AIDS* **1999**, *13*, 627−628.
(8) Schapiro, J. M.; Lawrence, J.; Speck, R.; Winters, M. A.; Efron, B.; Coombs, R. W.; Collier, A. C.; Merigan, T. C. *J. Infect. Dis.* **1999**, *179*, 249−253.
(9) Wainberg, M. A. *J. Am. Med. Assoc.* **1999**, *281*, 2169−2170.
(10) Vandamme, A. M.; Van Laethem, K.; De Clercq, E. *Drugs* **1999**, *57*, 337−361.
(11) Sarafianos, S. G.; Das, K.; Ding, J.; Boyer, P. L.; Hughes, S. H.; Arnold, E. *Chem. Biol.* **1999**, *6*, R137−R146.
(12) De Clercq, E. *Biochem. Pharmacol.* **1994**, *47*, 155−169.
(13) Macchi, B.; Mastino, A. *Pharmacol. Res.* **2002**, *46*, 473−482.

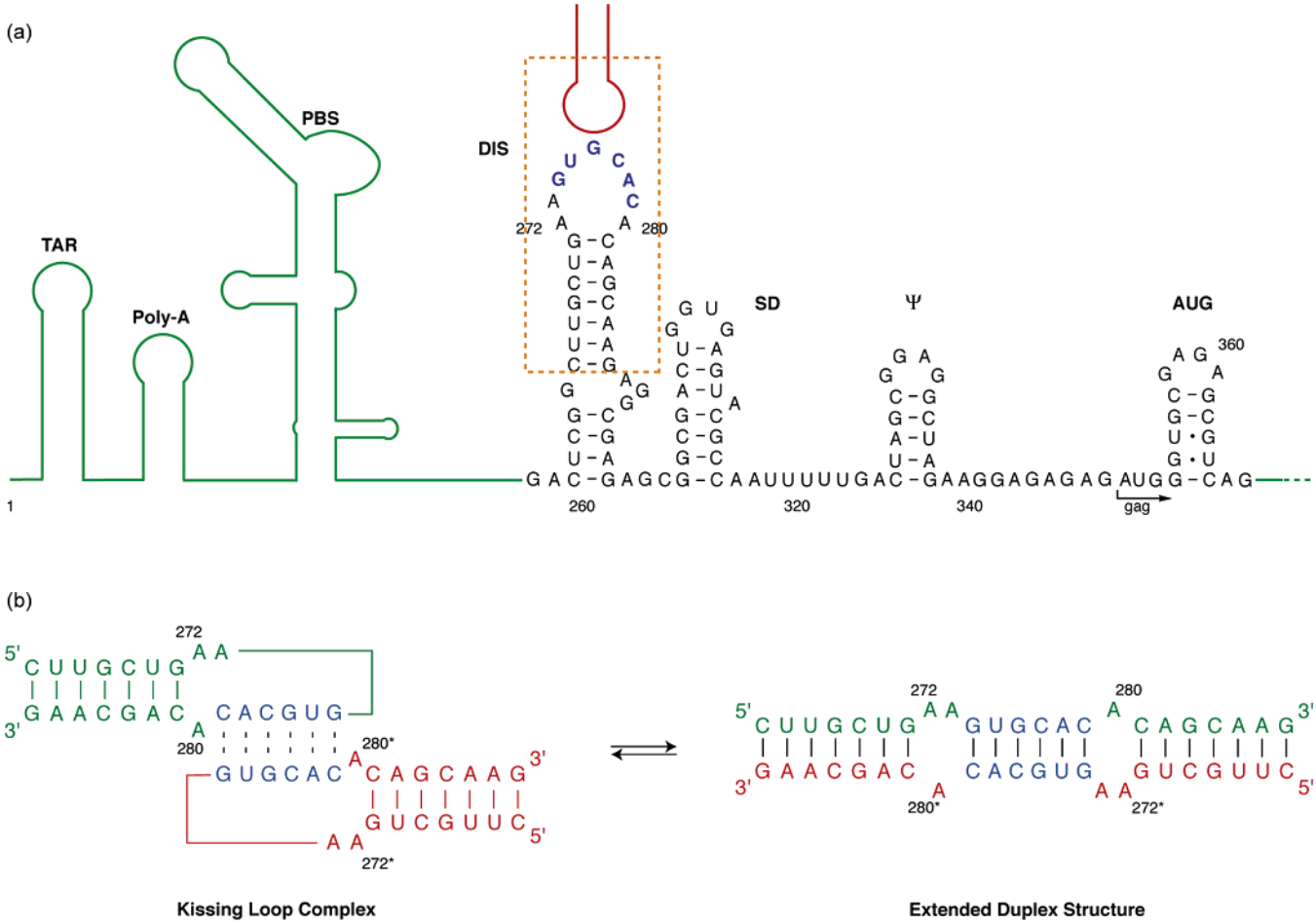

Figure 1. (a) Schematic representation of the 5′-end of the HIV RNA genome and the Dimerization Initiation Site (DIS) (orange box). The sequence of the Ψ-packaging region is explicitly shown. (b) Rearrangement of the DIS kissing-loop complex to an extended duplex structure (note the different orientation as compared to (a)). Strands are colored separately (red and green) as well as bases involved in kissing-loop base-pairing (blue). Abbreviations: TAR, *trans*-acting response element; poly-A, polyadenylation signal; PBS, primer-binding site; SD, major splice-donor site; Ψ (psi), main part of the RNA packaging signal; AUG, translation initiation codon of the *gag* gene.

all necessitate the continuous development of independent classes of anti-HIV drugs.[17,18] Additionally, recent disappointing results with experimental vaccines and the high cost of newly introduced drugs make the search for alternative and cheaper anti-HIV agents a scientific and social obligation.

As the successful replication of HIV requires an ordered pattern of viral gene expression,[19−21] several essential viral RNA binding proteins, particularly Tat and Rev, have recently become targets for drug design. Interfering with the sequence-specific interaction between these regulatory proteins and their respective viral RNA sites, TAR and RRE, has been explored as a potentially novel approach for antiretroviral therapy.[22−24] Discovery assays have been developed to identify low molecular weight ligands that can prevent the formation of these key viral RNA−protein complexes.[25−28]

An intriguing HIV-1 RNA target that has not been extensively explored for its therapeutic potential is the Dimerization Initiation Site (DIS).[29] In mature virus particles, the retroviral genome is noncovalently dimerized near its 5′-end. This dimeric nature has been demonstrated to be critically important for several key events in the life cycle of HIV, including reverse transcription and encapsidation.[30−32] The initial events leading to dimerization have been confined to stem loop 1 (SL1 or DIS), the first of four characterized stem loops found on the ca. 120 nt long HIV Ψ-packaging site (Figure 1a).[33,34] This conserved

(14) Claessens, Y. E.; Chiche, J. D.; Mira, J. P.; Cariou, A. *Crit. Care* **2003**, *7*, 226−232.
(15) Jost, S.; Bernard, M. C.; Kaiser, L.; Yerly, S.; Hirschel, B.; Samri, A.; Autran, B.; Goh, L. E.; Perrin, L. *N. Engl. J. Med.* **2002**, *347*, 731−736.
(16) Goulder, P. J.; Walker, B. D. *N. Engl. J. Med.* **2002**, *347*, 756−758.
(17) Check, E. *Nature* **2003**, *424*, 361.
(18) Gulick, R. M. *Clin. Microbiol. Infect.* **2003**, *9*, 186−193.
(19) Vaishnav, Y. N.; Wong-Staal, F. *Annu. Rev. Biochem.* **1991**, *60*, 577−630.
(20) Emerman, M.; Malim, M. H. *Science* **1998**, *280*, 1880−1884.
(21) Frankel, A. D.; Young, J. A. *Annu. Rev. Biochem.* **1998**, *67*, 1−25.
(22) Rosen, C. A.; Pavlakis, G. N. *AIDS* **1990**, *4*, 499−509.
(23) Cullen, B. R. *Microbiol. Rev.* **1992**, *56*, 375−394.
(24) Green, M. R. In *AIDS Research Reviews III*; Koff, W. C., Wong-Staal, F., Kennedy, R. C., Eds.; Marcel Dekker, Inc.: New York, 1993; pp 41−55.
(25) Zapp, M. L.; Stern, S.; Green, M. R. *Cell* **1993**, *74*, 969−978.
(26) Luedtke, N. W.; Tor, Y. *Angew. Chem., Int. Ed.* **2000**, *39*, 1788−1790.
(27) Lacourciere, K. A.; Stivers, J. T.; Marino, J. P. *Biochemistry* **2000**, *39*, 5630−5641.
(28) Luedtke, N. W.; Tor, Y. *Biopolymers* **2003**, *70*, 103−119.
(29) Ligand binding to the entire Ψ-packaging region has previously been studied. See: (a) McPike, M. P.; Goodisman, J.; Dabrowiak, J. C. *Bioorg. Med. Chem.* **2002**, *10*, 3663−3672. (b) McPike, M. P.; Sullivan, J. M.; Goodisman, J.; Dabrowiak, J. C. *Nucleic Acids Res.* **2002**, *30*, 2825−2831. (c) Sullivan, J. M.; Goodisman, J.; Dabrowiak, J. C. *Bioorg. Med. Chem. Lett.* **2002**, *12*, 615−618.
(30) Russell, R. S.; Liang, C.; Wainberg, M. A. *Retrovirology* **2004**, *1*, 23−36.
(31) Paillart, J. C.; Shehu-Xhilaga, M.; Marquet, R.; Mak, J. *Nat. Rev. Microbiol.* **2004**, *2*, 461−472.
(32) Berkhout, B.; van Wamel, J. L. *J. Virol.* **1996**, *70*, 6723−6732.
(33) Skripkin, E.; Paillart, J. C.; Marquet, R.; Ehresmann, B.; Ehresmann, C. *Proc. Natl. Acad. Sci. U.S.A.* **1994**, *91*, 4945−4949.

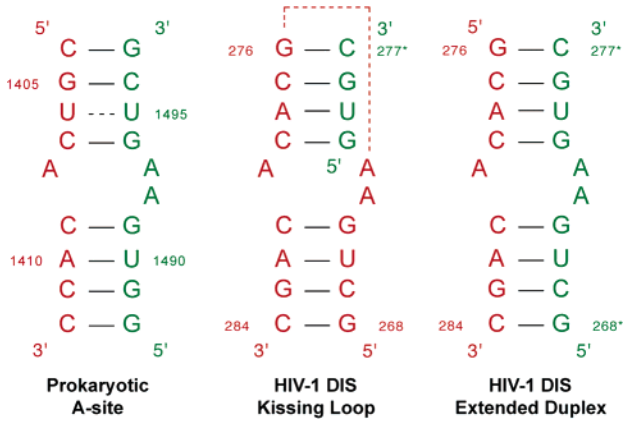

Figure 2. Similarity between the primary and secondary structures of the prokaryotic A-site, DIS kissing-loop complex, and DIS extended duplex structure. Subtype F of the HIV DIS is shown above and is characterized by bases A272, A273, and A280 that flank the loop sequence 5′-GUGCAC-3′. Subtype A, however, contains an A273G mutation with the same loop sequence as subtype F. Subtype B also contains flanking bases A272, A273, and A280 but is instead characterized by the loop sequence 5′-GCGCGC-3′.

stem loop RNA structure initiates dimerization by forming a "kissing loop", where six complementary nucleotides from each loop associate via base pairing. This kissing-loop complex can rearrange into a more stable extended duplex (Figure 1b).[35−37] Because mutations in the DIS have been shown to dramatically diminish viral infectivity,[38,39] small molecules that can disrupt or alter this essential process may constitute a viable antiretroviral therapeutic approach.[30] To learn about the recognition properties of HIV DIS in solution and to identify potential DIS binders, a "real-time" and sensitive assay is required. Here, we report the design, validation, and utilization of a novel fluorescence-based assay for the discovery and analysis of DIS binders using short oligonucleotides that reliably mimic the extended duplex structure found in viral particles.

Results

Design of Fluorescent RNA Oligonucleotides. Remarkable similarity between HIV DIS and the bacterial A-site has been recognized in the primary and secondary structures, for both the kissing loop and the extended duplex sequence arrangements (Figure 2).[40] A crystal structure reported by Ehresmann has shown the DIS to also exhibit notable three-dimensional resemblance to the prokaryotic ribosomal A-site.[40−42] In the bacterial A-site, the two dynamic A residues (1492 and 1493) are involved in the decoding process.[43−45] As has been shown in the NMR analyses of A-site models[46−48] and crystal structure analyses of whole 30S ribosomal subunits,[49,50] the conformationally flexible adenines are displaced from the interior of the RNA helix upon ligand binding.[47,51] Recent crystal structures show that purines A272 and A273 are also displaced and excluded from the interior of the DIS RNA helix upon binding of small molecules.[41,42] We therefore hypothesized that replacing one or two of these purine residues with an environmentally sensitive fluorescent nucleobase analogue, such as 2-aminopurine (2AP), may provide an effective reporting assay for DIS-ligand binding as has been demonstrated for the bacterial A-site.[52,53] This is schematically shown in Figure 3.

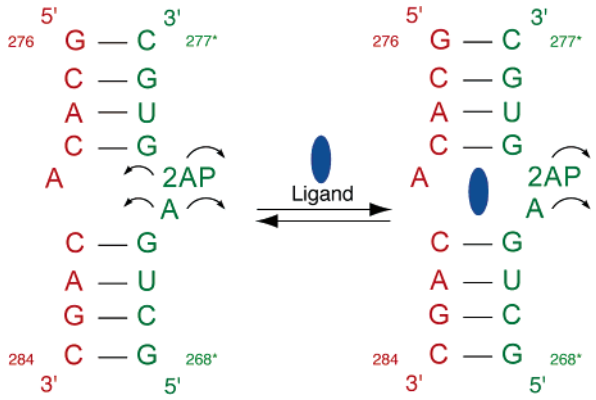

Figure 3. Putative base-flipping dynamics of purines 272 and 273 in the DIS extended duplex in analogy to the A-site. In the unbound state, purines 272 and 273 are presumed to freely rotate in and out of the helical domain. Upon ligand binding, purines 272 and 273 are displaced and forced out to the exterior of the DIS RNA helix.

Two minimized 23mer RNA constructs were designed to mimic the extended duplex structure of the HIV-1 DIS (subtype F) and to facilitate monitoring of small molecule binding to this site (Figure 4). Both RNA constructs, DIS272(2AP) and DIS273(2AP), contain 2AP that replaces purines A272 and A273, respectively, as a potential fluorescent reporter for small molecule binding.[54] A key question that needed to be addressed at the outset is whether or not the association of such short modified oligoribonucleotides can be controlled in solution.[55]

(34) Laughrea, M.; Jette, L. *Biochemistry* **1994**, *33*, 13464−13474.
(35) Huthoff, H.; Berkhout, B. *Biochemistry* **2002**, *41*, 10439−10445.
(36) Muriaux, D.; De Rocquigny, H.; Roques, B. P.; Paoletti, J. *J. Biol. Chem.* **1996**, *271*, 33686−33692.
(37) The mutifaceted process of viral RNA dimerization has been extensively studied by biochemical and biophysical methods. See, for example: (a) Mujeeb, A.; Clever, J. L.; Billeci, T. M.; James, T. L.; Parslow, T. G. *Nat. Struct. Biol.* **1998**, *5*, 432−436. (b) Jossinet, F.; Paillart, J. C.; Westhof, E.; Hermann, T.; Skripkin, E.; Lodmell, J. S.; Ehresmann, C.; Ehresmann, B.; Marquet, R. *RNA* **1999**, *5*, 1222−1234. (c) Lodmell, J. S.; Ehresmann, C.; Ehresmann, B.; Marquet, R. *J. Mol. Biol.* **2001**, *311*, 475−490. (d) Rist, M. J.; Marino, J. P. *Biochemistry* **2002**, *41*, 14762−14770. (e) Mihailescu, M. R.; Marino, J. P. *Proc. Natl. Acad. Sci. U.S.A.* **2004**, *101*, 1189−1194.
(38) Laughrea, M.; Jette, L.; Mak, J.; Kleiman, L.; Liang, C.; Wainberg, M. A. *J. Virol.* **1997**, *71*, 3397−3406.
(39) Shen, N.; Jette, L.; Liang, C.; Wainberg, M. A.; Laughrea, M. *J. Virol.* **2000**, *74*, 5729−5735.
(40) Ennifar, E.; Paillart, J. C.; Marquet, R.; Ehresmann, B.; Ehresmann, C.; Dumas, P.; Walter, P. *J. Biol. Chem.* **2003**, *278*, 2723−2730.
(41) Ennifar, E.; Paillart, J. C.; Bodlenner, A.; Walter, P.; Weibel, J. M.; Aubertin, A. M.; Pale, P.; Dumas, P.; Marquet, R. *Nucleic Acids Res.* **2006**, *34*, 2328−2339.
(42) Ennifar, E.; Dumas, P. *J. Mol. Biol.* **2006**, *356*, 771−782.
(43) Yoshizawa, S.; Fourmy, D.; Puglisi, J. D. *Science* **1999**, *285*, 1722−1725.
(44) Ogle, J. M.; Brodersen, D. E.; Clemons, W. M., Jr.; Tarry, M. J.; Carter, A. P.; Ramakrishnan, V. *Science* **2001**, *292*, 897−902.
(45) Kaul, M.; Barbieri, C. M.; Pilch, D. S. *J. Am. Chem. Soc.* **2006**, *128*, 1261−1271.
(46) Fourmy, D.; Recht, M. I.; Blanchard, S. C.; Puglisi, J. D. *Science* **1996**, *274*, 1367−1371.
(47) Fourmy, D.; Yoshizawa, S.; Puglisi, J. D. *J. Mol. Biol.* **1998**, *277*, 333−345.
(48) Yoshizawa, S.; Fourmy, D.; Puglisi, J. D. *EMBO J.* **1998**, *17*, 6437−6448.
(49) Carter, A. P.; Clemons, W. M.; Brodersen, D. E.; Morgan-Warren, R. J.; Wimberly, B. T.; Ramakrishnan, V. *Nature* **2000**, *407*, 340−348.
(50) Brodersen, D. E.; Clemons, W. M., Jr.; Carter, A. P.; Morgan-Warren, R. J.; Wimberly, B. T.; Ramakrishnan, V. *Cell* **2000**, *103*, 1143−1154.
(51) Vicens, Q.; Westhof, E. *Structure* **2001**, *9*, 647−658.
(52) Shandrick, S.; Zhao, Q.; Han, Q.; Ayida, B. K.; Takahashi, M.; Winters, G. C.; Simonsen, K. B.; Vourloumis, D.; Hermann, T. *Angew. Chem., Int. Ed.* **2004**, *43*, 3177−3182.
(53) Kaul, M.; Barbieri, C. M.; Pilch, D. S. *J. Am. Chem. Soc.* **2004**, *126*, 3447−3453.
(54) Note 2AP has previously been incorporated into the stem of shortened DIS constructs to monitor isomerization from the kissing loop to the extended duplex. See ref 37d.

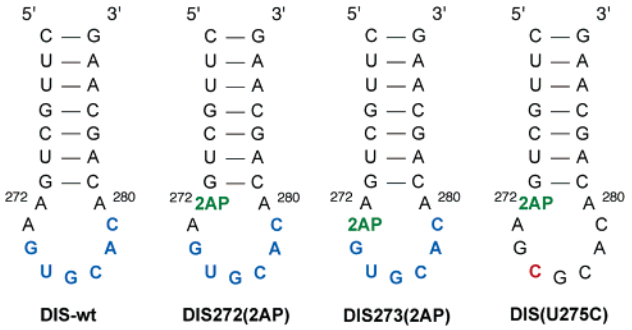

Figure 4. Sequence and secondary structure of 23mer RNA DIS constructs (subtype F). Constructs DIS272(2AP) and DIS273(2AP) are the fluorescently labeled RNA constructs, while DIS-wt is the wild-type sequence and DIS(U275C) is a non-dimerizing control sequence. Explicitly shown are the bases involved in the kissing-loop complex interaction (blue), 2-aminopurine (2AP, green), and the U275C mutation (red) that prevents kissing-loop complex formation.

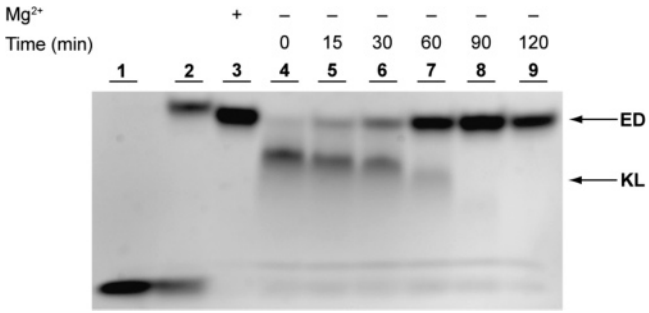

Figure 5. Native PAGE used to monitor the association of the RNA hairpins to a kissing loop (KL) and rearrangement to the extended duplex (ED). Lane 1: DIS(U275C) is a monomeric RNA hairpin control. Lane 2: DIS(U275C) was denatured and renatured to form an extended duplex. Lane 3: DIS272(2AP) was incubated for 2 h at 55 °C in the titration buffer to form an extended duplex structure. Lanes 4−9: DIS272(2AP) was denatured and incubated at 55 °C for 0, 15, 30, 60, 90, and 120 min, respectively, illustrating the thermal isomerization of the kissing-loop complex to extended duplex over time. See Materials and Methods for gel and buffer conditions.

Controlling Kissing Loop and Extended Duplex Formation. Knowledge of the specific state of the RNA (i.e., single stranded, kissing loop, or extended duplex) is essential for the interpretation of solution studies. To monitor the association and isomerization processes of the short DIS constructs, native polyacrylamide gel electrophoresis was employed (Figure 5). Several controls were first examined. DIS(U275C), a non-dimerizing RNA control sequence (Figure 4), serves as a negative control for marking the relative migration of a monomeric RNA hairpin (Figure 5, lane 1). Denaturation and renaturation of this construct results in the formation of an extended duplex (with traces of a monomeric oligonucleotide) as seen in lane 2. No kissing loop is ever observed with this mutant construct. As a positive control, the fluorescent construct

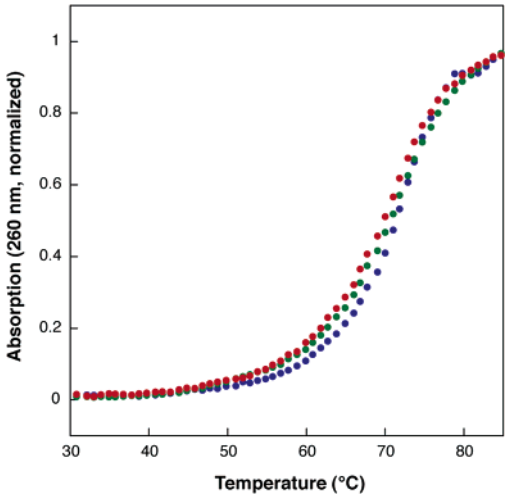

Figure 6. Normalized thermal melting profile of RNA constructs DIS-wt (blue), DIS272(2AP) (green), and DIS273(2AP) (red). See Materials and Methods for experimental details.

DIS272(2AP) was denatured and renatured in the presence of Mg^{2+}, followed by incubation for 2 h at 55 °C, which are the same conditions used for solution titrations, to generate the extended duplex (lane 3). The association of the construct was then more carefully scrutinized as a function of time in a similar buffer without Mg^{2+} to avoid extra-stabilization of the kissing-loop complex. Construct DIS272(2AP) was denatured at 90 °C and slowly renatured by incubation at 55 °C for 0, 15, 30, 60, 90, and 120 min (Figure 5, lanes 4−9, respectively). As the native gel reveals, the 2AP-modified RNA construct DIS272-(2AP) spontaneously forms a kissing loop upon heat denaturation, and then thermally rearranges into the extended duplex by incubation at 55 °C for an extended period of time (Figure 5). Because of the metastable nature of the kissing-loop complex,[35,56] all binding experiments discussed below were conducted after 2 h of equilibration to ensure the dominance of the stable extended duplex structure.

Thermal Denaturation Studies. To probe the impact of the 2AP substitution on the relative stability of the labeled DIS constructs, thermal denaturation experiments were performed. Figure 6 shows the melting curves of the 2AP-modified constructs DIS272(2AP) and DIS273(2AP) in comparison to the unmodified DIS-wt, all in their extended duplex form. Minimal perturbation on duplex stability is observed, as all three RNA constructs display nearly identical melting temperatures ($T_m \approx 72$ °C).[57] These results are consistent with previous observations illustrating that the incorporation of 2AP into nucleic acids has been reported to minimally disturb double helical structures.[52,58,59]

Monitoring RNA Small Molecule Binding to DIS Using DIS272(2AP). To determine if fluorescence intensity changes occur upon ligand binding to this minimized DIS construct, paromomycin (Figure 7a), a known DIS binder,[40] was initially

(55) Previous studies with other minimized RNA constructs have been utilized to mimic the kissing loop and extended duplex structure of the full-length viral genome. A 19 nt RNA consisting of a self-complementary loop and its flanking stem was shown to conform to a kissing-loop structure by NMR but not an extended duplex, see: (a) Dardel, F.; Marquet, R.; Ehresmann, C.; Ehresmann, B.; Blanquet, S. *Nucleic Acids Res.* **1998**, *26*, 3567−3571. However, the addition of two base-pairs to the stem reportedly stabilized the 23 nt construct to allow formation of a kissing loop as observed by 2D NMR, see: (b) Mujeeb, A.; Clever, J.; Billeci, T. M.; James, T. L.; Parslow, T. G. *Nat. Struct. Biol.* **1998**, *5*, 432−436. A 23 nt extended duplex was later reported by X-ray crystallography, see: (c) Ennifar, E.; Yusupov, M.; Walter, P.; Marquet, R.; Ehresmann, B.; Ehresmann, C.; Dumas, P. *Structure* **1999**, *7*, 1439−1449. Both structures appear to mimic the DIS secondary structure found in viral particles.

(56) Thermodynamic studies on the stability of DIS-type RNA loop−loop interactions have been reported. See: Weixlbaumer, A.; Werner, A.; Flamm, C.; Westhof, E.; Schroeder, R. *Nucleic Acids Res.* **2004**, *32*, 5126−5133. Lorenz, C.; Piganeau, N.; Schroeder, R. *Nucleic Acids Res.* **2006**, *34*, 334−342.

(57) Observed thermal melting points for DIS-wt, DIS272(2AP), and DIS273-(2AP) are 72 ± 0.6, 72 ± 0.6, and 70 ± 2.1 °C, respectively. See Materials and Methods for experimental details.

(58) Bradrick, T. D.; Marino, J. P. *RNA* **2004**, *10*, 1459−1468.

(59) Rist, M.; Marino, J. *Nucleic Acids Res.* **2001**, *29*, 2401−2408.

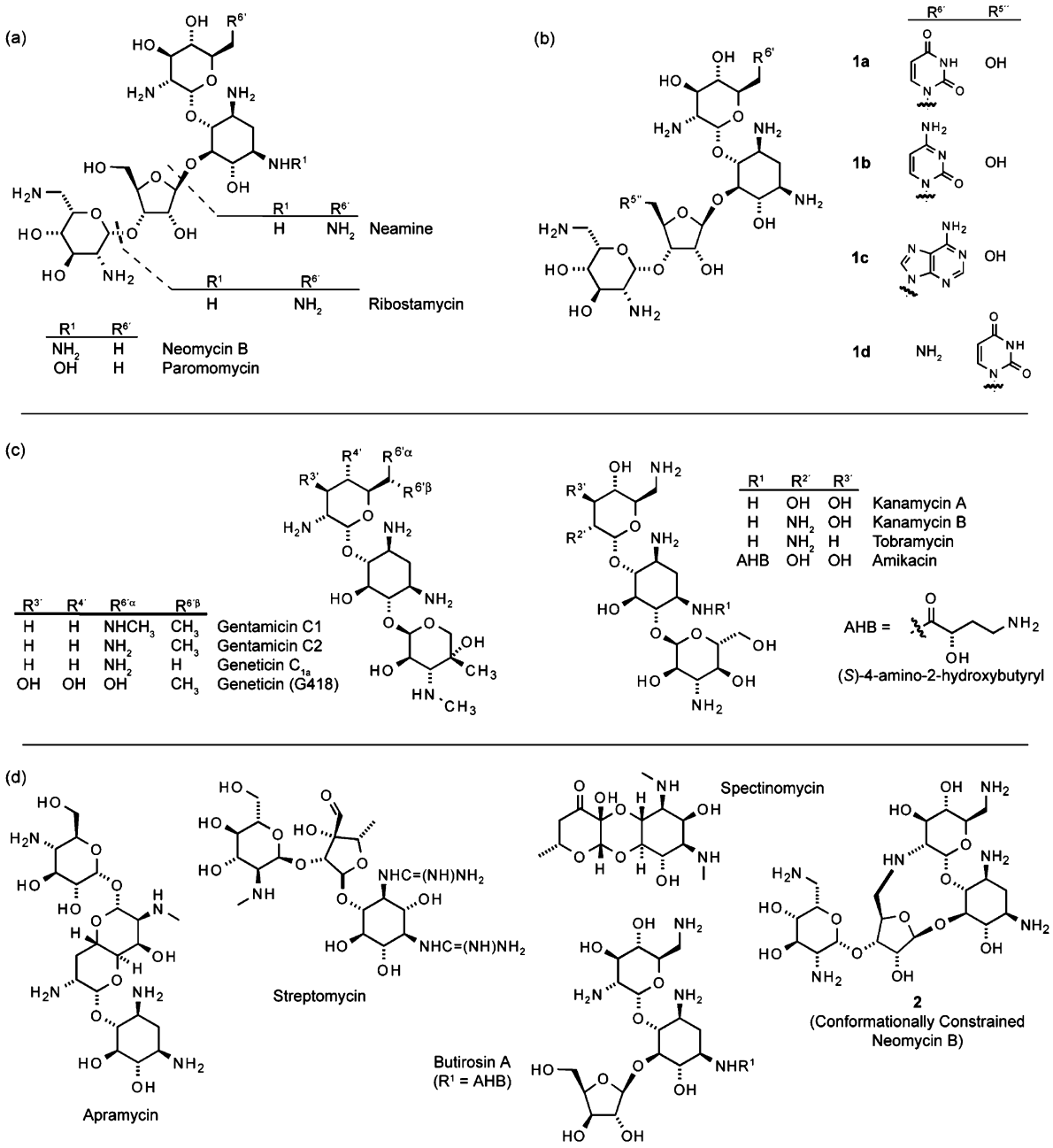

Figure 7. Structures of the different classes of ligands tested: (a) 4,5-disubstituted 2-DOS aminoglycosides; (b) semi-synthetic nucleobase−neomycin conjugates; (c) 4,6-disubstituted 2-DOS aminoglycosides; and (d) other related aminoglycoside antibiotics.

titrated into the 2AP-labeled construct DIS272(2AP). As shown in Figure 8a, when paromomycin is incrementally added to a solution of the folded RNA construct, a gradual increase in 2AP's emission intensity at 370 nm is observed. By titration's end, the fluorescence intensity of 2AP had increased over 300% (Figure 8c). A plot of normalized fluorescence intensity versus increasing concentrations of paromomycin yielded a binding isotherm characteristic of a dose−response curve (Figure 8d). Analysis of the curve yielded an EC_{50} value (the effective concentration at which 50% of the RNA is ligand bound) of 0.5 ± 0.2 μM.

Additional 4,5-disubstituted 2-deoxystreptamine (2-DOS) aminoglycosides were titrated and similarly evaluated, including neomycin B, ribstomycin, butirosin A, and neamine (Figure 7a). Table 1 lists the percent change in 2AP emission intensity for the free and ligand-bound 2AP-labeled DIS construct and the derived EC_{50} values for each aminoglycoside. When neomycin B, one of the strongest RNA binders, was titrated with DIS272-(2AP), a fluorescence intensity increase of over 150% was observed (see Supporting Information),[60] yielding affinity similar to that of paromomycin of approximately 0.6 ± 0.2 μM. Ribstomycin, a smaller three-ring antibiotic in the neomycin-family, was also screened for binding to the HIV-1 DIS. Despite the loss of ring IV, binding of ribstomycin caused a fluorescence intensity increase of over 100% with an EC_{50} value of 16.0 ± 4.0 μM. Butirosin A, a derivative of ribstomycin that contains an aminohydroxybutyryl (AHB) moiety attached to N1 of

(60) Note that studies with 2AP-labeled A-site have shown lack of correlation between affinity and fluorescence changes induced upon ligand binding. See ref 45.

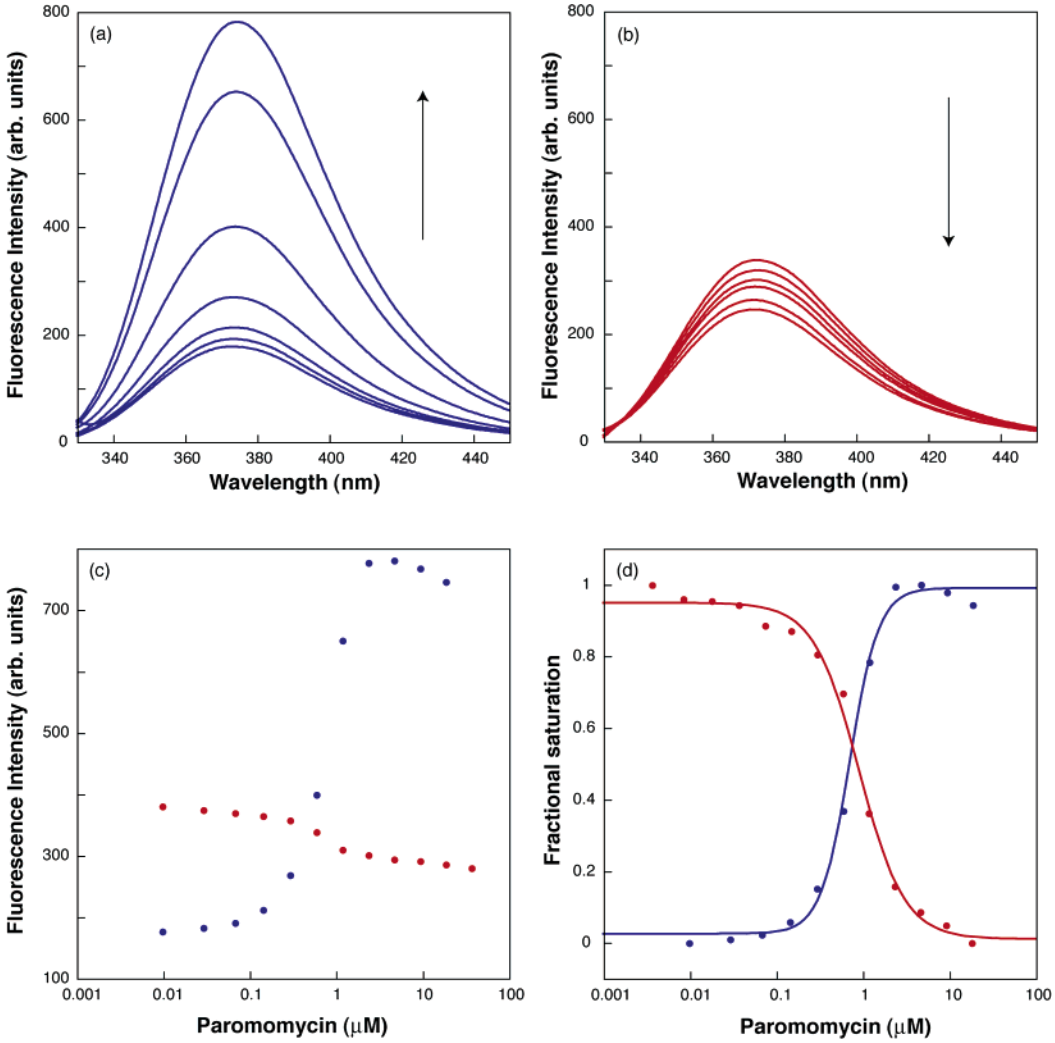

Figure 8. Fluorescence titrations of both 2AP-labeled DIS constructs with paromomycin. (a) Representative spectra of fluorescence intensity enhancement for DIS272(2AP) with increasing concentrations of paromomycin. (b) Representative spectra of fluorescence quenching for DIS273(2AP) with increasing concentrations of paromomycin. Note: Some intermediate spectra were omitted for clarity in both (a) and (b). (c) Comparison of absolute fluorescence intensity values of DIS272(2AP) (blue) and DIS273(2AP) (red) in the presence of increasing concentrations of paromomycin. (d) Comparison of normalized fluorescence intensity change for DIS272(2AP) (blue) and DIS273(2AP) (red) for paromomycin titrations. Note the similar EC_{50} values observed with both fluorescently labeled RNA constructs.

Table 1. Table of EC_{50} Values (μM) for DIS Ligand Binding[a]

	DIS272(2AP)		DIS273(2AP)	
ligand	EC_{50}[b]	% intensity change	EC_{50}	% intensity change
neamine	21.0 ± 1.2	+75%	12.3 ± 1.1	−30%
neomycin B	0.6 ± 0.2[c]	+150%	0.4 ± 0.03	−50%
paromomycin	0.5 ± 0.2[c]	+300%	0.9 ± 0.3	−25%
ribstomycin	16.0 ± 4.0	+100%	17.2 ± 2.6	−45%
apramycin	7.6 ± 1.0	+235%	6.1 ± 0.9	−35%
butirosin A	5.5 ± 0.6	+100%	n.a.[e]	n.a.
1a[d]	2.6 ± 1.1	+170%	n.a.	n.a.
1d[d]	2.2 ± 0.1	+265%	n.a.	n.a.
2[d]	1.9 ± 0.2[c]	+175%	1.5 ± 0.1	−35%

[a] See Materials and Methods for experimental details and Supporting Information for absolute fluorescence emissions curves. [b] EC_{50} values determined by a dose−response curve fit with $R > 0.99$. [c] Hill coefficients, $n \approx 2$, where for all other binders, $n \approx 1$. [d] Trifluoroacetate salt used instead of free amine. [e] Not applicable (n.a.); binding is not observed with DIS273(AP) construct.

ribstomycin, induced an intensity increase of over 100% with an EC_{50} value of 5.5 ± 0.6 μM. Neamine, with only rings I and II, was also titrated with DIS272(2AP). Known as the minimal motif necessary for binding to the analogous prokaryotic A-site, neamine also elicited a fluorescence intensity increase of nearly 75%. Its EC_{50} was determined to be 21.0 ± 1.2 μM. Neamine has been arbitrarily defined as the standard for "fluorescence change threshold" for this fluorescent RNA construct. Ligands that induce a weaker overall change in fluorescence intensity with this construct have been therefore considered as poor DIS binders and have not been studied any further.

Three neomycin B derivatives, previously reported by our laboratory as RNA binders,[61,62] were also discovered to effectively bind the HIV DIS construct. Uracil-conjugated neomycin **1a** (Figure 7b) elicited an intensity increase of nearly 170% upon binding to DIS272(2AP) with an EC_{50} value of 2.6 ± 1.1 μM. Conjugate **1d** with a uracil moiety at the 5″-position had a similar affinity (2.2 ± 0.1 μM) as that of **1a** but caused an intensity increase of over 265% upon binding to DIS272-(2AP). Other conjugates, containing adenine and cytosine at both positions (Figure 7b), were also screened; however, none showed

(61) Blount, K. F.; Zhao, F.; Hermann, T.; Tor, Y. *J. Am. Chem. Soc.* **2005**, *127*, 9818−9829.
(62) Blount, K. F.; Tor, Y. *ChemBioChem* **2006**, *7*, 1612−1621.

any evidence for binding through fluorescence changes. The conformationally constrained neomycin B analogue **2** (Figure 7d) caused an intensity increase of over 175% with a binding affinity of 1.9 ± 0.2 μM, approximately a 3-fold lower affinity as compared to that of neomycin or paromomycin.

Screening of other natural aminoglycosides outside the neomycin family suggests that 4,6-disubstituted 2-DOS aminoglycosides of the kanamycin family (Figure 7c) do not bind the DIS RNA. In addition, streptomycin and spectinomycin, two structurally unrelated aminoglycoside antibiotics (Figure 7d), have not shown any affinity to DIS using our fluorescent constructs. We have discovered, however, that apramycin, a structurally unique aminoglycoside, does bind the HIV-1 DIS (Figure 7d and Table 1). A fluorescence intensity increase of approximately 235% was observed upon binding with an EC_{50} value determined to be 7.6 ± 1.0 μM, a moderate affinity that is greater than that observed for ribstomycin or neamine.

Monitoring RNA Small Molecule Binding to DIS with DIS273(2AP). An additional fluorescent construct, where the 2AP modification has been placed in position 273 instead of 272, has been examined for its ability to monitor the binding of low molecular weight ligands to the DIS RNA. The ligands discussed above were also titrated with DIS273(2AP), and, unlike the increased emission observed for DIS272(2AP), a decrease in fluorescence intensity was observed. Addition of paromomycin to DIS273(2AP) resulted in an intensity decrease of approximately 25% when comparing the ligand-saturated to the unbound RNA (Figure 8b). Curve fitting of the binding isotherm determined the affinity of paromomycin to DIS273-(2AP) to be 0.9 ± 0.3 μM, similar to the affinity determined utilizing construct DIS272(2AP). Neomycin was subsequently titrated with DIS273(2AP) and induced a fluorescence decrease of over 50%. An EC_{50} of 0.4 ± 0.03 μM was determined and was again within experimental error of the affinity obtained for neomycin with the DIS272(2AP) construct. Similarly, titration of ribstomycin caused a decrease in the fluorescence intensity with final emission values at about 45% of the unbound DIS273(2AP). A moderate affinity of 17.2 ± 2.6 μM was obtained (Table 1), similar to the value determined with DIS272(2AP). Finally, neamine was titrated with the RNA construct, and a similar decrease in emission (ca. 30%), as detected with paromomycin, was observed upon ligand binding, yielding an affinity of 12.3 ± 1.1 μM for this core pharmacophore.

Interestingly, butirosin A and all of the nucleobase conjugates **1a**−**d** did not elicit any fluorescence change when titrated with DIS273(2AP). In contrast, both apramycin and the conformationally constrained neomycin analogue **2** induce measurable fluorescence changes when titrated into DIS273(2AP). Apramycin and **2** both elicited a 35% decrease in emission, yielding EC_{50} values of 6.1 ± 0.9 and 1.5 ± 0.1 μM, respectively. These affinities match well with the values obtained using DIS272-(2AP).

Discussion

Mimicking the HIV-1 DIS with Modified RNA Constructs. The ability of short oligonucleotides to structurally and functionally mimic larger RNA constructs has been established for the prokaryotic A-site.[63−68] The extraordinary similarity of the HIV-1 DIS to the bacterial A-site, both in the kissing loop and in the extended duplex arrangements, has therefore prompted us to explore the development of reporting RNA constructs that facilitate the study of the structural and recognition features of this intriguing RNA fold. Both constructs, DIS272(2AP) and DIS273(2AP), were based on previously reported short RNA constructs that were shown to mimic the kissing loop[69] and extended duplex[70] structure found in viral particles.[71]

Substitution of A272 and/or A273 with 2AP residues could have potentially disturbed the structure of the kissing complex and prevented its formation and consequent isomerization to the extended duplex. We have not observed such interference. Gel shift experiments have shown the effective formation of a kissing loop, and its rearrangement into the extended duplex, and thermal denaturation experiments have shown the 2AP-modified RNA constructs to be as stable as the wild-type DIS sequence. These observations can be rationalized by recent structural studies that have shown one or both purines (A272 or A273) to be bulging out of the RNA helix.[42] Substitution with 2AP at these dynamic and unpaired positions is therefore unlikely to significantly perturb the DIS construct's stability and its hybridization potential. Similar observations have been reported for the analogous bacterial A-site constructs.[52,53]

Fluorescent DIS Constructs Detect and Quantify Ligand Binding. In analogy to studies with the A-site RNA,[52,53] the fluorescent oligonucleotide sequences were selected to comprise the core DIS sequence and to retain the putative conformational flexibility of the two adenines 272 and 273 (Figure 2). In the model oligonucleotides DIS272(2AP) and DIS273(2AP), either adenine at position 272 or 273 has been replaced by 2AP, a fluorescent nucleoside that is highly sensitive to changes in its environment. Binding of specific ligands to the DIS construct was anticipated to induce changes in the fluorescence signal and provide "real-time" monitoring of ligand binding, because the bound ligand displaces the purines from the interior of the RNA and perturbs the immediate environment of the fluorescent probe. For the unbound DIS272(2AP) RNA, a low fluorescence intensity was observed, suggesting the purine at this position is significantly shielded within the DIS duplex. Upon ligand binding, a significant increase in the emission intensity of 2AP272 was observed, most likely due to the unstacking of 2AP and its rotation toward the helix exterior. In contrast, the unbound DIS construct DIS273(2AP) showed relatively high emission intensity, suggesting a rather exposed environment for the fluorescent probe in the ligand-free RNA. Ligand binding

(63) Recht, M. I.; Fourmy, D.; Blanchard, S. C.; Dahlquist, K. D.; Puglisi, J. D. *J. Mol. Biol.* **1996**, *262*, 421−436.
(64) Miyaguchi, H.; Narita, H.; Sakamoto, K.; Yokoyama, S. *Nucleic Acids Res.* **1996**, *24*, 3700−3706.
(65) Purohit, P.; Stern, S. *Nature* **1994**, *370*, 659−662.
(66) Wong, C. H.; Hendrix, M.; Priestley, E. S.; Greenberg, W. A. *Chem. Biol.* **1998**, *5*, 397−406.
(67) Griffey, R. H.; Hofstadler, S. A.; Sannes-Lowery, K. A.; Ecker, D. J.; Crooke, S. T. *Proc. Natl. Acad. Sci. U.S.A.* **1999**, *96*, 10129−10133.
(68) Lynch, S. R.; Puglisi, J. D. *J. Mol. Biol.* **2001**, *306*, 1037−1058.
(69) Ennifar, E.; Walter, P.; Ehresmann, B.; Ehresmann, C.; Dumas, P. *Nat. Struct. Biol.* **2001**, *8*, 1064−1068.
(70) Ennifar, E.; Yusupov, M.; Walter, P.; Marquet, R.; Ehresmann, B.; Ehresmann, C.; Dumas, P. *Structure* **1999**, *7*, 1439−1449.
(71) A related short 23mer RNA construct has been reported not to follow the two-state kissing-loop/extended duplex model because of its inability to form a kissing loop. This resulted from the presence of a G−U mismatch in the stem of the 23mer. See: Takahasi, K.; Baba, S.; Chattopadhyay, P.; Koyanagi, Y.; Tomamoto, N.; Takaky, H.; Kawai, G. *RNA* **2000**, *6*, 96−102.

results in modest fluorescence quenching for this RNA construct. Analogous to structural observations made with the A-site,[45,52,53] this decrease in emission can be attributed to partial stacking of 2AP273 onto the bulged out A272. While the two constructs respond differently to ligand binding, and the absolute changes in their emission are different, similar overall behavior is observed for both fluorescent constructs, suggesting the fluorescent probes monitor the same binding event.

Intriguingly, the corresponding 2AP-labeled A-site constructs exhibit a very similar behavior in terms of relative fluorescence emission intensities and impact of ligand binding upon 2AP emission. These observations suggest a high similarity between the conformations (and possibly the dynamic behavior) of A272/273 in DIS and A1492/1493 in the A-site, respectively. Both A272 and A1492 are observed to be partially buried within the duplex in the absence of any ligands and become more solvent exposed upon ligand binding. In contrast, A273 and A1493 are found to be more solvent exposed in the unbound state of the DIS and A-site. Ligand binding, in this case, causes stacking of the displaced residue upon the other bulged out purine, resulting in overall diminished emission. This previously unobserved solution behavior of DIS hints to yet another tier of resemblance between the two presumably unrelated RNA constructs.

For practical purposes, it is beneficial to use the DIS272-(2AP) construct, as it provides a signal enhancement upon specific ligand binding and a larger dynamic range. To differentiate between potent and nonspecific DIS binders, one needs to define the minimal change of fluorescence intensity to be viewed as a meaningful signal. We have selected the signal generated by neamine to be our threshold, as this two-ring ligand represents the minimal pharmacophore of most aminoglycosides. It is the smallest binder to display reasonable affinity to the DIS, inducing an approximate 75% increase in fluorescence intensity with the DIS272(2AP) construct. Paromomycin, a higher affinity binder, caused an increase in fluorescence intensity by over 300%, while neomycin having affinity similar to that of the DIS only induces a fluorescence intensity increase of 150% (Table 1). Ribstomycin, on the other hand, has a 15-fold lower affinity than either neomycin or paromomycin, but still elicits a 2-fold intensity increase comparable to neomycin (Table 1). This suggests that fluorescence intensity changes do not necessarily correlate with affinity and molecular size. This is not unprecedented, as similar observations have been made with 2AP-labeled A-site oligonucleotides, where neomycin, one of the strongest decoding site binders, does not elicit a significant fluorescence change.[45]

It is worth noting that for most molecules screened, a specific binding event was normally detected by both constructs DIS272-(2AP) and DIS273(2AP); however, with butirosin A and compounds **1a** and **1d**, a definitive binding event was only detected utilizing construct DIS272(2AP). In the absence of structural data for these DIS binders, it is difficult to rationalize these observations at the molecular level, as these derivatives may assume different binding modes. It is intriguing, however, to point out that all anomalously behaved derivatives contain modifications that protrude outside of the common aminoglycosidic skeleton. Butirosin A contains a 2-aminohydroxybutyryl side chain of the 2-deoxystreptamine (2-DOS) ring, and derivatives **1a** and **1d** possess a uracil residue conjugated at positions 6′ or 5″, respectively. It is plausible that these protrusions may abolish the environmental variations between the free and bound 2AP at position 273, resulting in very little emission intensity differences for the otherwise environmentally sensitive nucleobase.

Ligand Screening, Quantification, and New HIV-1 DIS Binders. Aminoglycosides of the neomycin family were the only known binders to the HIV-1 DIS (subtypes A and F),[40] and to date their affinity has not been reported.[72] Previous gel shift assays and footprinting experiments have shown the HIV-1 DIS to be a target for aminoglycosides, but the ability to quickly screen or quantify binding has been lacking. Based on our binding assay, ligands derived from the neomycin scaffold (both natural and semi-synthetic) successfully bind the fluorescent DIS constructs and elicit changes in 2AP emission. Comparing affinities generated by our DIS fluorescence assay to that obtained for the A-site using the corresponding 2AP-based assay shows good correlation. For example, the EC_{50} values for paromomycin,[52] one of the best DIS and A-site binders, are 0.5 ± 0.2 and 0.75 ± 0.05 μM, respectively. This suggests related binding modes in solution and corroborates recent structural analyses that show similar modes of binding for aminoglycosides of the neomycin/paromomycin family.

Rewardingly, our assay substantiates earlier observations suggesting undetectable binding of the kanamycin and tobramycin family to the DIS RNA site (Figure 7c).[40] These aminoglycosides bind well to the structurally related ribosomal A-site with low micromolar affinities.[67] The A-site is characterized by a non-canonical U1406−U1495 base pair (Figure 2), known to be essential for the activity of kanamycin, tobramycin, and related 4,6-disubstituted 2-DOS aminoglycosides. Substitution of U1406 for A in the A-site has indeed been shown to confer resistance against 4,6- but not 4,5-disubstituted 2-DOS aminoglycosides.[73] The DIS RNA, in contrast, contains a Watson−Crick base pair at the corresponding position (A282−U270*). It is this key difference that is likely to confer this unprecedented selectivity displayed by the DIS RNA for the 4,5- over the 4,6-disubstituted 2-DOS aminoglycosides (Figure 7a and c, respectively).

Screening additional natural aminoglycosides against our assay led to the discovery of apramycin, a structurally unique aminoglycoside (Figure 7d), as a new DIS binder (Table 1). The sequence difference between the A-site and DIS RNA outlined above, particularly the Watson−Crick base pairing at positions A282−U270*, is likely to facilitate the binding of apramycin to DIS. The U1406A mutation that replaces the non-canonical U·U pair in the A-site, while being detrimental to binding of the 4,6-disubstituted 2-DOS aminoglycosides, is known to confer a 4-fold hypersensitivity to apramycin.[74] Crystallographic and molecular modeling experiments[75] show a different orientation for apramycin within the bacterial decoding site and also suggest a U1406A mutation to be better accommodating for an A-site bound apramycin molecule. This would therefore support the observed affinity of apramycin to

(72) Affinities of aminoglycoside binding to the entire Ψ-packing region have been reported. See refs 29a−c.
(73) Pfister, P.; Hobbie, S.; Vicens, Q.; Bottger, E. C.; Westhof, E. *ChemBioChem* **2003**, *4*, 1078−1088.
(74) Recht, M. I.; Puglisi, J. D. *Antimicrob. Agents Chemother.* **2001**, *45*, 2414−2419.
(75) Han, Q.; Zhao, Q.; Fish, S.; Simonsen, K. B.; Vourloumis, D.; Froelich, J. M.; Wall, D.; Hermann, T. *Angew. Chem., Int. Ed.* **2005**, *44*, 2694−2700.

the DIS RNA that contains a Watson−Crick base pair at the analogous A282−U270* position.

Similarity between the HIV-1 DIS and the Bacterial A-Site. While the similarity between the HIV-1 DIS and the bacterial A-site in sequence, as well as in secondary and tertiary structure, has previously been recognized,[40] our solution studies shed light on the conformation and flexibility of the purine-rich bulge that represent the main ligand binding site. In particular, the parallel in relative fluorescence intensities and ligand-induced changes in the emission pattern of 2AP272/2AP273 in DIS with respect to 2AP1492/2AP1493, the analogous positions in the A-site, suggests highly similar conformational behavior in solution. This intriguing observation may be pertinent to future attempts to design DIS selective binders. On a positive note, the A-site has been recognized to be an encapsulating and therefore reasonably selective RNA target,[61] and attempts to design A-site selective ligands have met with some success.[76,77] This may translate to similar selectivity traits in the analogous HIV sequences, which is highly encouraging. A major challenge that remains to be addressed, however, is the inherently different pharmacokinetic properties that distinguish a bacterial A-site binder from a potential antiviral. In particular, aminoglycoside-based drugs are known to have favorable uptake properties into bacterial cells, while displaying rather poor uptake into mammalian cells.[78] The opposite behavior might need to be established to ensure selectivity and proper uptake into HIV infected mammalian cells.

Summary

The HIV-1 Dimerization Initiation Site (DIS) is a functionally important viral RNA target that can potentially be exploited for small molecule antiretroviral therapy.[30] To date, a limited number of reports have addressed the discovery of small molecule effectors that alter viral RNA dimerization. To a degree, this may have been due to the lack of convenient ways to establish ligand binding to DIS. To facilitate the assessment of its solution and recognition properties, two minimized fluorescent RNA constructs that simulate the behavior of the larger parent viral RNA have been synthesized and examined. The 23mer 2AP-labeled RNA constructs were found to self-associate to form metastable kissing loops that thermally rearrange into very stable extended duplexes containing two identical A-rich bulges. These conformationally flexible bulges serve as the recognition site for low molecular weight ligands of the aminoglycoside family of antibiotics. Binding events can be effectively followed by fluorescence spectroscopy where, depending on the labeling position, either enhancement or quenching of emission is observed.

Using the fluorescently labeled HIV-1 DIS constructs, we have made the following observations regarding ligand binding: (a) aminoglycosides of the neomycin family, such as paromomycin and neomycin B, show high affinity to the DIS RNA with submicromolar EC_{50} values, (b) aminoglycosides of the kanamycin family do not appear to bind the DIS RNA, (c) apramycin, a naturally occurring and structurally unique aminoglycoside, binds DIS with low micromolar affinity and represents a novel, previously unobserved scaffold for DIS recognition, and (d) semi-synthetic aminoglycoside analogues such as conformationally constrained neomycin B and nucleobase−aminoglycoside conjugates bind DIS with relatively high affinity, albeit lower than the parent unmodified aminoglycosides. The fluorescent DIS constructs, in addition to proving extremely useful in analyzing ligand binding, have yielded valuable information on the conformational state of the short RNA oligonucleotides. We have observed high similarity between the HIV-1 DIS and the bacterial decoding A-site, both in their solution ligand binding behavior, and particularly in the intra- and extra-helical residence of the conformationally flexible A residues within the bulge. This resemblance is likely to facilitate the design of new DIS selective ligands as potential antiretroviral agents.

Materials and Methods

General. For gel electrophoresis, thermal denaturation studies, sources and purification of aminoglycosides, as well as synthesis and preparation of RNA oligonucleotides, see the Supporting Information.

Fluorescence Binding Assay. For binding experiments, DIS constructs were refolded by heating a 25 μM solution of the 2AP-labeled DIS in a cacodylate binding buffer (2.0×10^{-2} M sodium cacodylate, pH 7.0, 2.5×10^{-2} M KCl, 2.0×10^{-3} M $MgCl_2$) to 90 °C for 2 min, followed by flash cooling on ice for 2 min. The kissing loop conformation was favored under these conditions. DIS constructs were incubated for 2 h at 55 °C and slowly cooled to room temperature to obtain the extended duplex. RNA constructs were quantified in 50 mM Na_3PO_4 (pH 7.5) with the following extinction coefficient (260 nm) values (in units of cm^{-1}/M^{-1}): DIS-wt ($\epsilon = 225\,500$), DIS-(U275C) ($\epsilon = 212\,900$), DIS272(2AP) ($\epsilon = 216\,200$), DIS273(2AP) ($\epsilon = 216\,400$). For all fluorescence measurements, a Perkin-Elmer LS50B fluorimeter was used, with an excitation slit width of 15 nm and an emission slit width of 20 nm. Upon excitation at 310 nm, the spectrum between 315 and 500 nm (scan rate of 300 nm/min) was recorded.

In a typical binding experiment, the fluorescence spectrum of a 120 μL solution of the buffer in the absence of any RNA or aminoglycoside was recorded. This spectral blank, for which only Raman scatter was observed, was subtracted from all subsequent spectra within each binding experiment. Following determination of the buffer blank, 5 μL of a 25 μM solution of refolded, 2AP-labeled DIS was added (final concentration is 1 μM), the solution mixed, and the spectrum again recorded. Subsequent aliquots of 1 μL of an aqueous aminoglycoside solution (increasing concentrations from 1 μM to 10 mM) and the fluorescence spectrum were recorded after each aliquot until the 2-aminopurine fluorescence reached saturation. Over the entire range of aminoglycoside concentrations, the emission maximum at 370 nm did not significantly vary (<1.0 nm). No "background emission" was observed near 370 nm. As small, concentrated volumes of aminoglycosides were titrated in, the total volume of the sample never changed more than 10%.

EC_{50} values were calculated through a four-parameter nonlinear curve fit using Kaleidagraph with a floating Hill slope coefficient (eq 1) where fractional change in emission intensity was taken as the fraction of aminoglycoside bound (χ). The calculated fractional saturation to derive the effective concentration at which 50% of aminoglycoside (AG) is bound (EC_{50}) to the DIS RNA follows:

$$\chi_{\text{bound}} = y_{\min} + \left(\frac{y_{\max}[\text{AG}]^n}{[\text{EC}_{50}]^n + [\text{AG}]^n} \right) \quad (1)$$

(76) Hermann, T.; Tor, Y. *Expert Opin. Ther. Pat.* **2005**, *15*, 49−62.
(77) Zhou, Y. F.; Gregor, V. E.; Sun, Z. X.; Ayida, B. K.; Winters, G. C.; Murphy, D.; Simonsen, K. B.; Vourloumis, D.; Fish, S.; Froelich, J. M.; Wall, D.; Hermann, T. *Antimicrob. Agents Chemother.* **2005**, *49*, 4942−4949.
(78) Luedtke, N. W.; Carmichael, P.; Tor, Y. *J. Am. Chem. Soc.* **2003**, *125*, 12374−12375.

where n is the Hill coefficient or degree of cooperativity associated with binding.

Acknowledgment. We thank Dr. Kenneth Blount for the nucleobase−aminoglycoside conjugates **1a**−**1d**, and Dr. Fang Zhao for supplying the conformationally constrained neomycin B analogue **2**. We are grateful to Prof. Cristina Bellucci for assistance with assay development and Prof. Thomas Hermann for insightful discussions. We are indebted to the University-wide AIDS Research Program Predoctoral Fellowship (D04-SD-409 to V.T.) and the National Institutes of Health (grant numbers AI 47673 and GM 069773 to Y.T.) for support.

Supporting Information Available: General methods, fluorescence emission spectra for DIS272(2AP) and DIS273(2AP) in the presence of each DIS binder, along with normalized binding isotherms. This material is available free of charge via the Internet at http://pubs.acs.org.

JA0675797